

# A nonlinear voice from GW250114 ringdown

Yi-Fan Wang , <sup>\*</sup> Sizheng Ma  Neev Khera  and Huan Yang , <sup>†</sup>

<sup>1</sup>*Max-Planck-Institut für Gravitationsphysik (Albert-Einstein-Institut), Am Mühlenberg 1, D-14476 Potsdam, Germany*

<sup>2</sup>*Perimeter Institute for Theoretical Physics, Waterloo, ON N2L2Y5, Canada*

<sup>3</sup>*Department of Physics, University of Guelph, Guelph, Ontario, Canada N1G 2W1*

<sup>4</sup>*Department of Astronomy, Tsinghua University, Beijing 100084, China*

The detection of quadratic quasi-normal modes would provide a direct probe into black hole nonlinear perturbations. We report the first observational evidence of a set of quadratic quasi-normal modes in the gravitational-wave ringdown of a binary black hole merger. Analyzing the signal from GW250114, we detect six nonlinear modes from the quadratic coupling of the fundamental (2,2,0) mode and its first two overtones. At 5 final mass ( $M_f$ ) after the merger, the evidence for these nonlinear modes reaches a Bayes factor of 74. To single out these contributions, we employ recent theoretical progress to compute the waveforms and subtract the corresponding nonlinear modes from a numerical relativity surrogate waveform. Our data analysis uses a novel method that incorporates inspiral-merger inference results as a highly constraining prior for the ringdown inference. We further perform a test allowing for phenomenological deviations for the theoretically predicted amplitudes of the quadratic modes. The results show that an amplitude of zero is excluded at  $3.0\sigma$  significance level, while the theoretical expectation is consistent with the inference. This detection marks a first step towards observationally characterizing nonlinear perturbations in the ringdown of a black hole.

## I. INTRODUCTION

The gravitational waves (GWs) emission during the black hole ringdown phase contains a superposition of damped sinusoidal signals, known as quasi-normal modes (QNMs) [1]. According to the no-hair theorem [2–4], the frequencies and damping times of these modes are uniquely determined by the mass and spin of the remnant black hole. Detecting multiple QNMs thus enables independent inference of the black hole’s mass and spin and verification of the no-hair theorem. This approach, often termed black hole spectroscopy [5, 6], offers a means to test general relativity (GR) in the strong-field regime surrounding a Kerr black hole. Beyond the linear QNM spectrum, there are additional non-modal signals [7, 8], tail [9–12], dynamical excitation, and nonlinearities present in the ringdown. For example, quadratic modes [13–17] arise from second-order perturbation and provide a direct probe into the nonlinear dynamics of GR. Detecting such quadratic modes is thus crucial for understanding the full theoretical structure of black hole perturbation.

Extracting the rich QNM spectrum in the ringdown signals poses data analysis challenges, partly due to the need to isolate the ringdown phase from the preceding inspiral and merger phases. A variety of strategies have been developed to address this issue, including time- or frequency-domain methods [18–32]. Historically, the first observational evidence of a fundamental  $(\ell, m, n) = (2, 2, 0)$  QNM, where  $\ell, m$  are the polar and azimuthal numbers and  $n$  denotes the overtone number, came from the first detection in GW150914 [33] and has

since been further probed in subsequent events [34–36]. Evidence of a subdominant fundamental mode (3,3,0) was reported by Ref. [19] from GW190521 [37, 38], attributed to the large remnant mass and asymmetric mass ratio; an alternative interpretation accounting for (2,1,0) modes in the presence of precessing spins is discussed in [39]. More recently, GW231123 exhibited evidence of modes beyond the dominant (2,2,0) QNM [40, 41], but its complex source properties established difficulty on mode identification. Additionally, [42] reported a detection of the overtone (2,2,1) in GW150914 by starting the analysis at the merger time.

However, starting the ringdown analysis close to the merger present significant data analysis challenges given the current incomplete theoretical understanding of the involved components. This regime involves a complex mixture of additional overtones [43, 44], non-modal signals (e.g., direct waves [7]), and nonlinearities such as quadratic modes [13–17]. Without a theoretical framework, it is difficult to cleanly separate these contributions in a data-driven approach, especially when multiple modes are comparable in amplitude without clear hierarchical ordering. These challenges will become more pronounced in high signal-to-noise ratio (SNR) events. Nevertheless, enabled by recent theoretical progress [17], we focus on detecting and isolating nonlinear quadratic modes by computing their amplitudes and subtracting this contribution from the overall signal.

The previous ringdown analysis commonly excises the pre-ringdown data [18–24] or model it in an agnostic way [25]. However, in principle, the amplitude and phase of each QNM are determined by the pre-ringdown dynamics. As the evidence grows in GR’s accuracy in describing the full waveform from binary black hole coalescence, the inspiral and merger phase should, in turn, provide informative constraints for ringdown analysis [45, 46]. In this work, we introduce a novel methodology that integrates

<sup>\*</sup> [yifan.wang@aei.mpg.de](mailto:yifan.wang@aei.mpg.de)

<sup>†</sup> [hyangdoa@tsinghua.edu.cn](mailto:hyangdoa@tsinghua.edu.cn)

information from the pre-ringdown data analysis. This is achieved by isolating the likelihood contribution from the inspiral-merger phase and ringdown phase, respectively, by gating and inpainting [19, 21, 47, 48] data outside the region of interest. The posterior of the inspiral-merger phase is folded into the ringdown analysis as an informed prior to boost the detectability. This approach makes use of the inspiral-merger inference results while simultaneously ensuring an independent ringdown data analysis.

We apply this method to the black hole merger event GW250114, the loudest GW detection to date with a network matched-filtering SNR of 80 [49, 50] by LIGO [51], Virgo [52] and KAGRA [53] collaboration. The source is consistent with a binary of nearly equal-mass with small spins. Previous analysis [49, 50] have reported evidence for the fundamental QNM (2, 2, 0) and its first overtone (2, 2, 1). Building on this, we extend the investigation to the quadratic QNMs within the (4, 4) multiple. The coupling ratio between quadratic and linear modes is calculated theoretically. The amplitudes of the linear modes are determined by a least-square fitting against `NRSur7dq4` [54], a numerical relativity surrogate waveform. This approach ensures a unified set of parameters to describe both the inspiral-merger and ringdown stages, thus we do not introduce any additional free parameters in the ringdown inference. By subtracting the quadratic modes from (4, 4), we establish a procedure to quantify their detection significance within a set of other signals. The corresponding Bayes factor reaches 74 when evaluated from  $5 M_f$  after the merger. We also perform a test by introducing a fractional deviation to the amplitude of the quadratic QNMs from the theoretical computation, and find that the inference is consistent with the theoretical prediction. A zero amplitude of the quadratic QNMs is excluded with significance of  $3.0 \sigma$ .

## II. METHOD

At the core of our data analysis is the integration of the inference results from inspiral-merger phase to inform ringdown analysis. Such a prior from inspiral and merger imposes strong constraints; for instance, in the limit of infinite SNR during the inspiral-merger phase, we can predict the QNM spectrum with arbitrary precision, thus providing an exact prior. As a result, this method enhances our detectability of sub-dominant QNM modes, provided the ringdown data are consistent with the theoretical expectation.

We formalize this approach within a Bayesian framework for parameter estimation and model selection. According to the Bayes theorem, the posterior probability distribution of parameters  $\vartheta$  given data  $d$  is

$$p(\vartheta|d) = \frac{\mathcal{L}(d|\vartheta)\pi(\vartheta)}{\mathcal{Z}(d)} \quad (1)$$

where  $\mathcal{L}(d|\vartheta)$  is the likelihood,  $\pi(\vartheta)$  is the prior and  $\mathcal{Z}(d)$  is the evidence. The Bayes factors are defined as a ratio

between evidences from two competing models. We propose a composite likelihood following [48, 55] that cleanly separates the contributions from the inspiral-merger (IM) phase and the ringdown (R) phase

$$\mathcal{L}(\{d_{\text{IM}}, d_{\text{R}}\}|\vartheta) = \mathcal{L}_{\text{IM}}(d_{\text{IM}}|\vartheta) \times \mathcal{L}_{\text{R}}(d_{\text{R}}|\vartheta) \quad (2)$$

The factorization is made possible by splitting the entire inspiral-merger-ringdown data series  $d$  into two disjoint segments,  $d_{\text{IM}}$  and  $d_{\text{R}}$ , using a gating-and-inpainting technique [19, 21]. Consequently, the total Bayesian evidence also factorizes:

$$Z(\{d_{\text{IM}}, d_{\text{R}}\}) = Z(d_{\text{IM}}) \times Z(d_{\text{R}}). \quad (3)$$

The joint posterior can be reformulated as

$$p(\vartheta|\{d_{\text{IM}}, d_{\text{R}}\}) = \frac{\mathcal{L}_{\text{R}}(d_{\text{R}}|\vartheta) \times \Pi(\vartheta|d_{\text{IM}})}{Z(d_{\text{R}})} \quad (4)$$

where we define the informed prior  $\Pi(\vartheta|d_{\text{IM}})$  as the posterior distribution obtained from the inspiral-merger analysis:

$$\Pi(\vartheta|d_{\text{IM}}) = \frac{\mathcal{L}(d_{\text{IM}}|\vartheta) \times \pi(\vartheta)}{Z(d_{\text{IM}})}. \quad (5)$$

In essence, we use gating and inpainting to isolate the likelihood contributions, then utilize the inspiral-merger inference results as a physically-motivated, informative prior for the subsequent ringdown-only analysis.

Given the nearly equal-mass nature of GW250114, our analysis targets the nonlinear QNMs within the (4, 4) multiple. As the detection of high SNR events becomes increasingly common, ringdown analysis faces a general challenge of isolating individual contributions within a set of signals, particularly at early times close to the merger, when multiple components coexist without a clear hierarchy of dominance. In this work, we address this by systematically computing the amplitudes of a set of six nonlinear quadratic modes, generated from the coupling of any two linear (2, 2,  $n$ ) QNMs, where  $n \in \{0, 1, 2\}$ , and then subtracting them from (4, 4) mode to measure their significance.

The inspiral and merger phases are modeled using `NRSur7dq4`, which includes all multiples up to  $\ell = 4$ . The characteristic frequency and damping time of each QNM are derived from the remnant mass and spin predicted by `NRSur7dq4`, while the corresponding amplitudes and phases of the linear (2, 2,  $n$ ) modes are obtained via a least-squares fit (see Section A) to the (2, 2) multiple. Consequently, the free parameters  $\vartheta$  in this analysis are precisely those that determine `NRSur7dq4`, including the binary masses, spins, sky location, source orientation, polarization, and merger time, introducing no additional degrees of freedom for the ringdown.

Wave-wave interactions produce nonlinearities in the black hole ringdowns. While the tail signal is generically small and the direct wave primarily matters in the merger stage before  $5 M_f$  [8], the interaction of QNMs should

dominate after that point. At second-order for the  $(4, 4)$  multiple produced by non-precessing systems, they lead to quadratic modes [15, 16] as

$$\begin{aligned} & \sum_{n,m} rA_{22n \times 22m} e^{-i\omega_{22n \times 22m} t} \\ &= \sum_{n,m} \mathcal{R}_{22n \times 22m}(a_f) \times rA_{22n} \times rA_{22m} e^{-i\omega_{22n} t} e^{-i\omega_{22m} t} \end{aligned} \quad (6)$$

where  $rA$  is the product of the source distance and the amplitude is measured in unit of  $M_f$ . The subscripts  $22n \times 22m$  refer to the quadratic QNM from coupling between the two parent linear QNMs  $(2, 2, n)$  and  $(2, 2, m)$ . The coupling coefficient  $\mathcal{R}_{22n \times 22m}$  depends on the remnant spin  $a_f$ . For non-precessing binaries, this ratio is computed using the methods outlined in [16] (summarized in Section C) and illustrated in Fig. 1

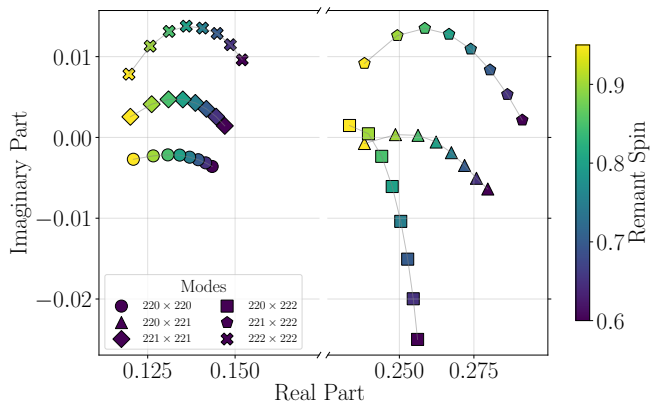


FIG. 1: The coupling coefficient  $\mathcal{R}_{22n \times 22m}$  from different coupling channels as a function remnant spin, obtained by solving the reduced second-order Teukolsky equation through a hyperboloidal slicing [16].

Ideally, for a given starting time, it is preferable to include infinite (overtone) mode sum in Eq. (6) to completely characterize second-order mode couplings. In practice, there are only finite linear modes that can be extracted from data with sufficiently accurate amplitude, i.e. a truncation has to be applied. Similarly to the linear mode case, higher-overtone modes become more relevant at earlier times. For a truncated series of modes at a starting time (e.g.  $5 M_f$ ), we can estimate the relative importance of residual quadratic modes if the mode-coupling coefficients are known.

For a ringdown analysis relevant for GW250114, we can faithfully predict the amplitudes of  $(2, 2, n)$  when  $n \leq 2$  based on least-square fitting towards NRSur7dq4 (see the convergence test in Section B), so that the series can be truncated up to  $(2, 2, 2)$ , i.e. a set of six quadratic modes available. We can theoretically address the importance of remaining quadratic modes at  $5 M_f$  by using the numerical relativity simulation SXS:BBH:3617 [56],

an equal-mass, non-spinning binary that is representative of GW250114. By fitting the next overtone  $(2, 2, 3)$  from the numerical simulation, we theoretically compute the residual modes coming from  $(2, 2, 3) \times (2, 2, n)$  where  $n \leq 3$ . It turns out that at  $5 M_f$ , these four modes contribute to a signal that is approximately 15% of the SNR of the first six modes. By contrast, considering only one quadratic mode involving  $(2, 2, 0)$ , or three quadratic modes involving  $(2, 2, 1)$  would significantly change the signal as shown in Fig. 2. This is an indication that the first six modes are already a major part of all quadratic modes at this time.

We further consider the residual between the  $(4, 4)$  multiple and six quadratic QNMs. Using the sum of the linear modes  $(4, 4, 0)$  and  $(4, 4, 1)$  obtained through a least-square fit towards the residual, the sum of all QNMs achieves a match to 97%, while not including quadratic modes can only achieve a match 89% with the linear modes. A comparison between the complete  $(4, 4)$  signal and our quadratic-mode reconstruction is shown in Fig. 2, together with a fit with only linear or adding quadratic QNMs being shown in the inset. In addition, a divergent mode-sum (as is known for linear modes, e.g. [57]) often leads to abrupt changes from the total signal, which is not observed at this starting time. It suggests that  $5 M_f$  is a qualified starting time for linear and nonlinear mode analysis for this system.

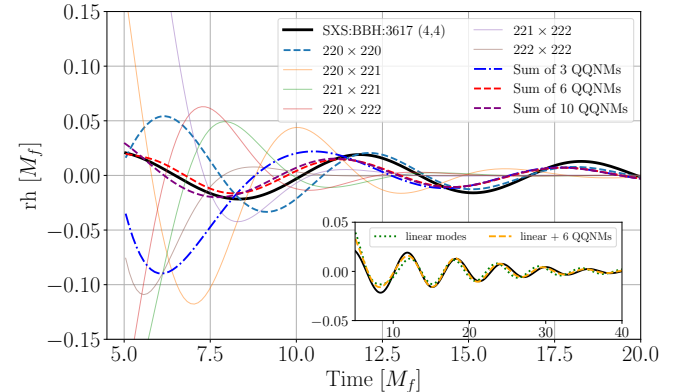


FIG. 2: Comparison of the  $(4, 4)$  multiple of the numerical relativity simulations SXS:BBH:3617 and various quadratic modes. The sum of 3, 6 and 10 quadratic QNMs involves overtone couplings up to  $(2, 2, 1)$ ,  $(2, 2, 2)$  and  $(2, 2, 3)$ , respectively. In the inset plot, we show a fit using only the linear  $(4, 4, 0)$  and  $(4, 4, 1)$  modes, where the match achieves 89%. A fit by further adding the 6 quadratic modes would increase the match to 97%.

### III. DATA ANALYSIS WITH GW250114

We analyze the interval  $[-6, 2]$  s of data [58–60] centered on the merger time of GW250114 using PyCBC

Inference [61] in addition to the padding time at both ends of the data. To cleanly separate the inspiral-merger and ringdown phase, we apply gating and inpainting with durations of 2 and 1 s, removing inspiral and ringdown when analyzing the other region, respectively. The sky location and merger time are fixed to the maximum-likelihood values reported in [49, 50], with right ascension and declination (ra, dec) = (2.35, 0.22) rad and the merger GPS time 1420878141.2362 s. The polarization angle is fixed to 1.37 rad. We use the `dynesty` [62] sampler with 30000 live points to sample the posterior distribution and stop when the change of logarithm of Bayesian evidence is less than 0.1. Priors are chosen as follows: the chirp mass and mass ratio have a prior uniform in the source-frame component masses, the spins follow an isotropic distribution with uniform amplitude up to 0.3, as guided by the inference results of small spins in [49, 50], the distance is assigned a prior uniform in the comoving volume, and the source orientation is isotropic. We explore a range of transition times between the inspiral-merger and ringdown segments, discretized from 3 to 9  $M_f$  relative to the merger time of GW250114, in steps of 1  $M_f$ .

At times less than 5  $M_f$  to the merger, additional non-modal signals can interfere with a clean least-square fit for the linear (2, 2,  $n$ ) modes. We therefore reconstruct these modes only at later start times, between 6 and 10  $M_f$ , and extrapolate the resulting amplitudes backward to earlier times. In practice, we sample from a Gaussian distribution whose mean and variance are estimated from the multiple extrapolated values, thereby marginalizing over the uncertainties in the reconstruction. A consistency test for fits from multiple times is shown in Section B.

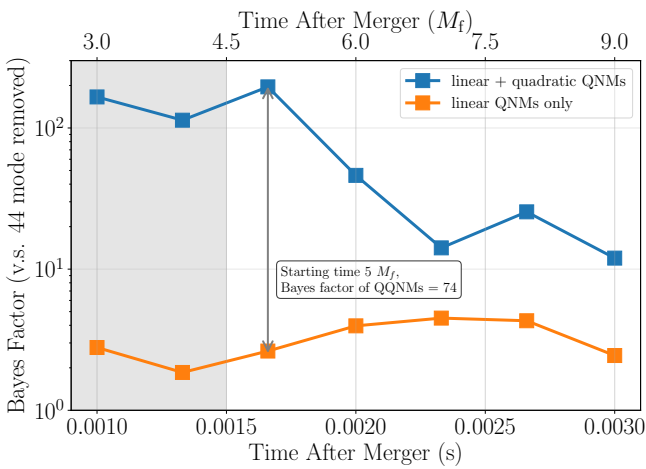


FIG. 3: Bayes factors comparing two ringdown models against a baseline that removes the (4, 4) mode. Starting at 5  $M_f$ , the full model including both linear and quadratic QNMs is favored with a Bayes factor of 74 compared with the linear-only model.

To quantify the contribution of the quadratic modes,

we construct two competing ringdown models: a linear-mode model, obtained by subtracting the sum of the six quadratic modes from the (4, 4) multiple, i.e.,  $h_{44} \rightarrow h_{44} - h_{\text{QQNM}}$ ; and a nonlinear model, which retains the full (4, 4) multiple. As a reference, we also define a baseline model that entirely removes the (4, 4) from `NRSur7dq4`. The Bayes factor between the nonlinear- and linear-mode models provides the detection significance for the existence of nonlinear quadratic modes.

In Fig. 3, we present the Bayes factors for each competing model relative to the baseline. At a start time of 5  $M_f$  after the merger, a model that incorporates all six quadratic QNMs is favored with a Bayes factor of 74. Within 3 to 9  $M_f$ , removing quadratic modes would all lower the Bayes factors. To further visualize our hierarchical Bayes inference, the whitened strain data and the maximum-likelihood waveform for the inspiral-merger phase and the ringdown phase transitioned at 5  $M_f$  are shown in Fig. 4.

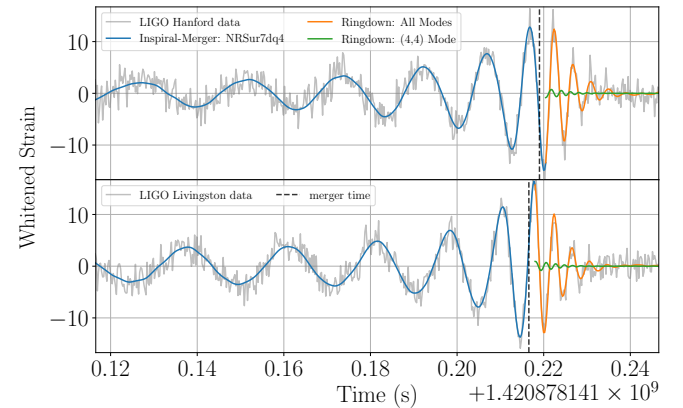


FIG. 4: Whitened data and maximum-likelihood waveform model for the ringdown analysis starting at 5  $M_f$  after the merger.

The quadratic mode represents a crucial non-linear GR effect in the black hole ringdown. Given its physical importance, we test the consistency of its amplitude with the theoretical prediction by introducing a fractional deviation parameter  $\delta A$ , defined through modifying the (4, 4) multiple by  $h_{44} \rightarrow h_{44} - \delta A \times h_{\text{QQNM}}$ . A value of  $\delta A = 0$  corresponds to agreement with theoretical expectation, and  $\delta A = 1$  corresponds to the scenario with no quadratic modes. As shown in Fig. 5, at 5  $M_f$ , the posterior for  $\delta A$  is  $-2.1_{-2.2}^{+1.14}$  (90% credible interval), with the theoretical value at the 1% quantile. While the peak of posterior is offset from 0, the entire posterior is broad to encompass the theoretical value, thus we conclude a consistency with the prediction of GR theory. Importantly, a zero amplitude is excluded with a significance of 3.0  $\sigma$ . This analysis provides the first observational evidence for the existence of quadratic modes, establishing a new direct probe of nonlinear GR effects in black hole ringdown.

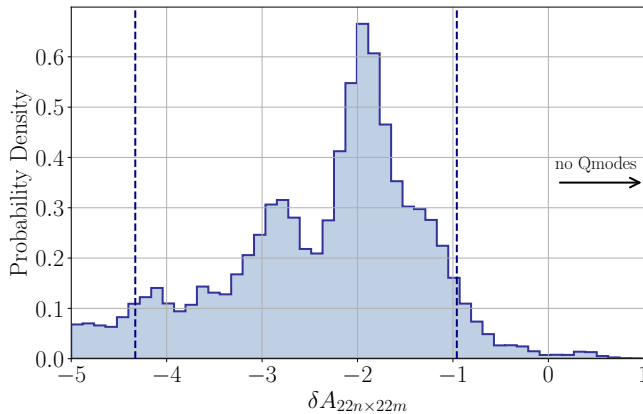


FIG. 5: Posterior distribution for the fractional deviation  $\delta A$  of the quadratic mode amplitudes from the theoretical prediction. The dashline represents the 90% credible interval. A zero amplitude of quadratic modes is excluded with  $3.0\sigma$ . The theoretical expectation value consistent with the posterior at the 1% quantile.

#### IV. DISCUSSION AND CONCLUSIONS

In this work, we report the detection of a set of six quadratic QNMs involving the coupling between  $(2, 2, 0)$ ,  $(2, 2, 1)$ , and  $(2, 2, 2)$  in the ringdown signal of GW250114. By incorporating information from the inspiral-merger phase into the ringdown analysis, we obtain a Bayes factor of 74 in favor of the quadratic mode model starting at  $5 M_f$  after the merger. This analysis provides the first observational evidence for the excitation of quadratic modes in the remnant of a binary black hole merger. We establish a framework to separate quadratic modes from a superposition of multiple components close to the merger by theoretically computing their contributions. The inference of the amplitude of the quadratic mode shows no deviation from theoretical expectations under a phenomenologically parametrized deviation, and the zero-quadratic-mode scenario is ruled out with a significance of  $3.0\sigma$ .

Our work introduces a new ringdown analysis approach using the posterior from the inspiral-merger phase as an informed prior for the ringdown analysis. This strategy enhances the detectability of subdominant ringdown modes by providing more constraining information from the pre-ringdown phase.

Several future developments could further improve this framework. These include marginalizing over the ringdown start time to better assess systematic uncertainties using methods such as those in [48, 55], though such an approach requires a more complicated computation, thus beyond the scope of the current work. In this work we assume the align spin symmetry between the  $+/-m$  mode in the ringdown, which is proper for GW250114 in light of its consistency with zero spin, but this can be extended to consider spin precessing in the future [63].

Extending the analysis to earlier times will require modeling additional nonlinearities, such as the direct wave contribution [7, 8] and the dynamic excitation of modes. Applying the present method to additional events and combining evidence by stacking [64] will also help detect fainter ringdown signals and improve the constraints on potential deviations from GR. The current parameterization for testing GR employs a simple fractional deviation and assumes a GR prior for the inspiral-merger phase, this framework can be refined in light of improved theoretical models.

The detection of quadratic QNMs in GW250114 marks a milestone that allows the identification of nonlinearities in a perturbed black hole. Future observations are expected to detect a richer set of modal and non-modal, linear and nonlinear signatures in the ringdown. While this poses significant challenges for both the theoretical studies and data analysis, it offers tremendous potential in understanding the fundamental predictions of GR in the strong-field regime.

All data analysis results and scripts necessary to reproduce this work are released in <https://github.com/yi-fan-wang/nonlinear-ringdown-GW250114>.

#### ACKNOWLEDGMENTS

The computational work for this manuscript was carried out on the Hypatia computer cluster at the Max Planck Institute for Gravitational Physics (Albert Einstein Institute) in Potsdam. YFW thanks Collin Capano and Alex Correia for their development of the hierarchical model in PyCBC, which this work employs to integrate inspiral-merger inference with ringdown analysis, thanks Qian Hu for reviewing this manuscript in the LIGO Publications & Presentations system, and thanks the Ringdown Inside and Out meeting organized by the Strong group at the Niels Bohr Institute, where the collaboration of this project was initiated. This research has made use of data or software obtained from the Gravitational Wave Open Science Center (gwosc.org), a service of the LIGO Scientific Collaboration, the Virgo Collaboration, and KAGRA. This material is based upon work supported by NSF's LIGO Laboratory which is a major facility fully funded by the National Science Foundation, as well as the Science and Technology Facilities Council (STFC) of the United Kingdom, the Max-Planck-Society (MPS), and the State of Niedersachsen/Germany for support of the construction of Advanced LIGO and construction and operation of the GEO600 detector. Additional support for Advanced LIGO was provided by the Australian Research Council. Virgo is funded, through the European Gravitational Observatory (EGO), by the French Centre National de Recherche Scientifique (CNRS), the Italian Istituto Nazionale di Fisica Nucleare (INFN) and the Dutch Nikhef, with contributions by institutions from Belgium, Germany, Greece, Hungary, Ireland, Japan, Monaco, Poland, Portugal, Spain. KAGRA is supported

by Ministry of Education, Culture, Sports, Science and Technology (MEXT), Japan Society for the Promotion of Science (JSPS) in Japan; National Research Foundation (NRF) and Ministry of Science and ICT (MSIT) in Korea; Academia Sinica (AS) and National Science and Technology Council (NSTC) in Taiwan. Research at Perimeter Institute is supported in part by the Government of Canada through the Department of Innovation, Science and Economic Development and by the Province of Ontario through the Ministry of Colleges and Universities.

### Appendix A: Least Square Fitting

The least square fitting is used to obtain the amplitude of  $(2, 2, n)$  QNM overtones from an inspiral-merger-ringdown numerical simulation or its surrogate model. Consider a model composed of multiple QNMs:

$$h(t) = \sum_{k=1}^M A_k e^{-i\omega_k t}, \quad (\text{A1})$$

where  $A_k$  is the complex amplitude of the  $k$ -th mode,  $\omega_k$  is the known complex frequency, and  $M$  is the total number of modes.

Given the targeted data  $d(t_n)$  at  $N$  time points, we define the sum of squared residuals

$$R = \sum_{n=1}^N \left| d(t_n) - \sum_{k=1}^M A_k e^{-i\omega_k t_n} \right|^2. \quad (\text{A2})$$

The objective is to obtain a fit of the complex amplitudes  $A_k$  to minimize  $R$ . Define the data vector  $\mathbf{d}$ , amplitude vector  $\mathbf{A}$ , and matrix  $\mathbf{G}$

$$\mathbf{d} = [d(t_1) \ d(t_2) \ \cdots \ d(t_N)]^T, \quad (\text{A3})$$

$$\mathbf{A} = [A_1 \ A_2 \ \cdots \ A_M]^T, \quad (\text{A4})$$

$$\mathbf{G} = \begin{bmatrix} e^{-i\omega_1 t_1} & e^{-i\omega_2 t_1} & \cdots & e^{-i\omega_M t_1} \\ e^{-i\omega_1 t_2} & e^{-i\omega_2 t_2} & \cdots & e^{-i\omega_M t_2} \\ \vdots & \vdots & \ddots & \vdots \\ e^{-i\omega_1 t_N} & e^{-i\omega_2 t_N} & \cdots & e^{-i\omega_M t_N} \end{bmatrix}, \quad (\text{A5})$$

where the superscript  $T$  denotes transpose. The QNM waveform can be compactly written as

$$\mathbf{h} = \mathbf{G}\mathbf{A}. \quad (\text{A6})$$

The sum of squared residuals can be expressed as

$$R = (\mathbf{d} - \mathbf{G}\mathbf{A})^H (\mathbf{d} - \mathbf{G}\mathbf{A}), \quad (\text{A7})$$

where the superscript  $H$  denotes the conjugate transpose. Taking the derivative with respect to the complex conjugate  $\mathbf{A}^H$  and setting it to zero

$$\frac{\partial R}{\partial \mathbf{A}^H} = -\mathbf{G}^H \mathbf{d} + \mathbf{G}^H \mathbf{G} \mathbf{A} = 0, \quad (\text{A8})$$

we obtain the solution

$$\mathbf{A} = (\mathbf{G}^H \mathbf{G})^{-1} \mathbf{G}^H \mathbf{d}. \quad (\text{A9})$$

### Appendix B: Consistency Test for Amplitude Extraction of the $(2, 2, n)$ modes

To validate the consistency of the extraction of QNM amplitudes, we construct the mode across multiple starting times with the numerical relativity surrogate model `NRSur7dq4` by least square fitting. We consider a  $(30, 30)$   $M_\odot$  binary with zero spin which is representative of GW250114, and extract the  $(2, 2, n)$  QNMs ( $n \leq 2$ ) at multiple starting times from 6 to 10  $M_f$  after the merger. The extract amplitudes are then extrapolated back to 5  $M_f$ , the reference time adopted in this work to report the detection of a set of six quadratic QNMs. The extrapolation employs a sinusoid QNM model, with decay times determined from the remnant mass and spin under the Kerr black hole scenario.

The faithfulness of the extrapolated amplitudes at 5  $M_f$  is quantified by the ratio of the standard variance to the mean. As shown in Fig. 6, the standard variance for the  $(2, 2, 0)$ ,  $(2, 2, 1)$  and  $(2, 2, 2)$  modes is only 0.1%, 1% and 6% of their respective mean amplitudes. These results demonstrate that the extrapolated amplitudes at 5  $M_f$  are robust against variations in the start time of fitting, thereby validating the reliability of the amplitude extraction procedure.

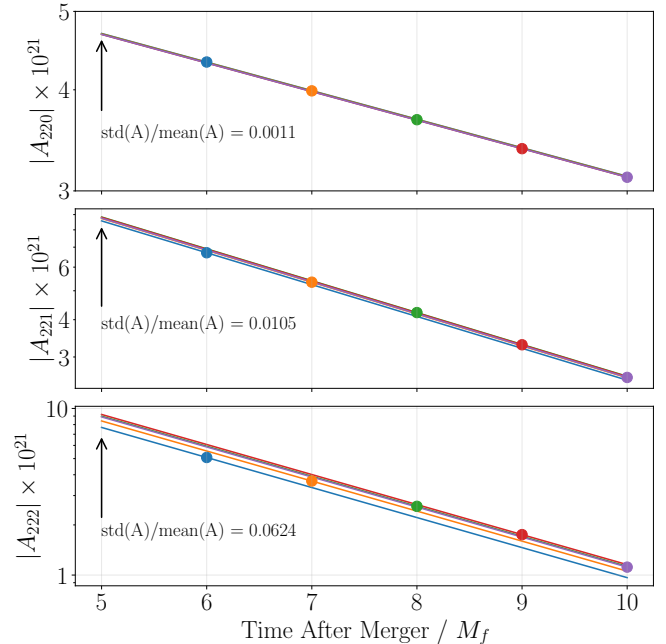


FIG. 6: The dots and solid lines are the fitted and extrapolated amplitudes, respectively, for  $(2, 2, n)$  modes ( $n \leq 2$ ). Each color represents a different starting time of the fit from 6 to 10  $M_f$  after the merger. The amplitudes extrapolated to 5  $M_f$  (left end of each curve) show good consistency across different starting times, indicating a faithful reconstruction. The ratios between the standard variance (std) and the mean of the extrapolated amplitudes are shown.

### Appendix C: A brief introduction to the computation of quadratic QNM coupling coefficients

Given a pair of QNMs with frequencies  $\omega_1$  and  $\omega_2$  with azimuthal numbers  $m_1$  and  $m_2$ , at second order in perturbation theory these QNMs produce quadratic modes with frequencies  $\omega_1 + \omega_2$ ,  $\omega_1 - \bar{\omega}_2$ , and  $-\bar{\omega}_1 + \omega_2$  and azimuthal numbers  $m_1 + m_2$ ,  $m_1 - m_2$  and  $-m_1 + m_2$  respectively. The excitation of the combination  $-\bar{\omega}_1 - \bar{\omega}_2$  happens to vanish.

Note that in addition for every QNM with frequency  $\omega_1$ , there is another QNM with frequency  $-\bar{\omega}_1$ , which we call its conjugate mode. For example, the prograde  $(2, 2, 0)$  and prograde  $(2, -2, 0)$  QNMs are conjugate modes whose frequencies are related as above. Consequently, any given quadratic frequency component can be generated by up to 3 combinations of QNM pairs. For instance,  $\omega_{220} + \omega_{221}$  frequency component is generated by the products of the prograde modes  $(2, 2, 0) \times (2, 2, 1)$ ,

$(2, 2, 0) \times (2, -2, 1)$  and  $(2, -2, 0) \times (2, 2, 1)$ . The amplitude of this frequency component will be given by

$$A_{220 \times 221} = \mathcal{R}_{++} A_{220} A_{221} + \mathcal{R}_{+-} A_{220} A_{2-21} + \mathcal{R}_{-+} A_{2-20} A_{221} \quad (C1)$$

However, if the system has reflection symmetry about the  $z$ -axis, such as for non-precessing systems, this relation simplifies significantly. The amplitude  $A_{\ell mn}$  of the prograde  $(\ell, m, n)$  mode is related to the prograde amplitude  $A_{\ell(-m)n}$  of the prograde  $(\ell, -m, n)$  mode by  $A_{\ell mn} = (-1)^\ell \bar{A}_{\ell(-m)n}$ . This allows us to combine all three contributions into a single amplitude ratio, which is used in this paper.

The individual Ratios  $\mathcal{R}_{++}$ ,  $\mathcal{R}_{+-}$  and  $\mathcal{R}_{-+}$  are computed using the methods in [16], which uses pseudospectral methods on a hyperboloidal slicing to perform metric reconstruction for the QNMs, compute the second order source term and solve the reduced second order Teukolsky equation. See [16] for more details.

---

[1] C. V. Vishveshwara, Scattering of gravitational radiation by a schwarzschild black-hole, *Nature* **227**, 936 (1970).

[2] W. Israel, Event horizons in static vacuum space-times, *Phys. Rev.* **164**, 1776 (1967).

[3] W. Israel, Event horizons in static electrovac space-times, *Communications in Mathematical Physics* **8**, 245 (1968).

[4] B. Carter, Axisymmetric black hole has only two degrees of freedom, *Phys. Rev. Lett.* **26**, 331 (1971).

[5] O. Dreyer, B. J. Kelly, B. Krishnan, L. S. Finn, D. Garrison, and R. Lopez-Aleman, Black hole spectroscopy: Testing general relativity through gravitational wave observations, *Class. Quant. Grav.* **21**, 787 (2004), arXiv:gr-qc/0309007.

[6] E. Berti *et al.*, Black hole spectroscopy: from theory to experiment, (2025), arXiv:2505.23895 [gr-qc].

[7] N. Lu, S. Ma, O. J. Piccinni, Y. Chen, and L. Sun, GW250114 reveals black hole horizon signatures, (2025), arXiv:2510.01001 [gr-qc].

[8] N. Oshita, S. Ma, Y. Chen, and H. Yang, Probing Direct Waves in Black Hole Ringdowns, (2025), arXiv:2509.09165 [gr-qc].

[9] S. Ma, M. A. Scheel, J. Moxon, K. C. Nelli, N. Deppe, L. E. Kidder, W. Throwe, and N. L. Vu, Merging black holes with Cauchy-characteristic matching: Computation of late-time tails, *Phys. Rev. D* **112**, 024003 (2025), arXiv:2412.06906 [gr-qc].

[10] M. De Amicis *et al.*, Late-time tails in nonlinear evolutions of merging black holes, (2024), arXiv:2412.06887 [gr-qc].

[11] T. Islam, G. Fagioli, G. Khanna, S. E. Field, M. van de Meent, and A. Buonanno, Phenomenology and origin of late-time tails in eccentric binary black hole mergers, *Phys. Rev. D* **112**, 024061 (2025), arXiv:2407.04682 [gr-qc].

[12] M. De Amicis, S. Albanesi, and G. Carullo, Inspiral-inherited ringdown tails, *Phys. Rev. D* **110**, 104005 (2024), arXiv:2406.17018 [gr-qc].

[13] K. Mitman *et al.*, Nonlinearities in Black Hole Ringdowns, *Phys. Rev. Lett.* **130**, 081402 (2023), arXiv:2208.07380 [gr-qc].

[14] M. H.-Y. Cheung *et al.*, Nonlinear Effects in Black Hole Ringdown, *Phys. Rev. Lett.* **130**, 081401 (2023), arXiv:2208.07374 [gr-qc].

[15] S. Ma and H. Yang, Excitation of quadratic quasinormal modes for Kerr black holes, *Phys. Rev. D* **109**, 104070 (2024), arXiv:2401.15516 [gr-qc].

[16] N. Khera, S. Ma, and H. Yang, Quadratic Mode Couplings in Rotating Black Holes and Their Detectability, *Phys. Rev. Lett.* **134**, 211404 (2025), arXiv:2410.14529 [gr-qc].

[17] N. Khera, A. Ribes Metidieri, B. Bonga, X. Jiménez Forteza, B. Krishnan, E. Poisson, D. Pook-Kolb, E. Schnetter, and H. Yang, Nonlinear Ringdown at the Black Hole Horizon, *Phys. Rev. Lett.* **131**, 231401 (2023), arXiv:2306.11142 [gr-qc].

[18] G. Carullo, W. Del Pozzo, and J. Veitch, Observational Black Hole Spectroscopy: A time-domain multimode analysis of GW150914, *Phys. Rev. D* **99**, 123029 (2019), [Erratum: Phys. Rev. D 100, 089903 (2019)], arXiv:1902.07527 [gr-qc].

[19] C. D. Capano, M. Cabero, J. Westerweck, J. Abedi, S. Kastha, A. H. Nitz, Y.-F. Wang, A. B. Nielsen, and B. Krishnan, Multimode Quasinormal Spectrum from a Perturbed Black Hole, *Phys. Rev. Lett.* **131**, 221402 (2023), arXiv:2105.05238 [gr-qc].

[20] M. Isi and W. M. Farr, Analyzing black-hole ringdowns, (2021), arXiv:2107.05609 [gr-qc].

[21] Y.-F. Wang, C. D. Capano, J. Abedi, S. Kastha, B. Krishnan, A. B. Nielsen, A. H. Nitz, and J. Westerweck, Gating-and-inpainting perspective on GW150914 ringdown overtone: Understanding the data analysis systematics, *Phys. Rev. D* **112**, 083023 (2025), arXiv:2310.19645 [gr-qc].

[22] S. Ma, K. Mitman, L. Sun, N. Deppe, F. Hébert, L. E. Kidder, J. Moxon, W. Throwe, N. L. Vu, and Y. Chen, Quasinormal-mode filters: A new approach to analyze the gravitational-wave ringdown of binary black-hole mergers, *Phys. Rev. D* **106**, 084036 (2022), arXiv:2208.07380 [gr-qc].

arXiv:2207.10870 [gr-qc].

[23] S. Ma, L. Sun, and Y. Chen, Using rational filters to uncover the first ringdown overtone in GW150914, *Phys. Rev. D* **107**, 084010 (2023), arXiv:2301.06639 [gr-qc].

[24] S. Ma, L. Sun, and Y. Chen, Black Hole Spectroscopy by Mode Cleaning, *Phys. Rev. Lett.* **130**, 141401 (2023), arXiv:2301.06705 [gr-qc].

[25] E. Finch and C. J. Moore, Frequency-domain analysis of black-hole ringdowns, *Phys. Rev. D* **104**, 123034 (2021), arXiv:2108.09344 [gr-qc].

[26] R. Brito, A. Buonanno, and V. Raymond, Black-hole Spectroscopy by Making Full Use of Gravitational-Wave Modeling, *Phys. Rev. D* **98**, 084038 (2018), arXiv:1805.00293 [gr-qc].

[27] A. Ghosh, R. Brito, and A. Buonanno, Constraints on quasinormal-mode frequencies with LIGO-Virgo binary-black-hole observations, *Phys. Rev. D* **103**, 124041 (2021), arXiv:2104.01906 [gr-qc].

[28] E. Maggio, H. O. Silva, A. Buonanno, and A. Ghosh, Tests of general relativity in the nonlinear regime: A parametrized plunge-merger-ringdown gravitational waveform model, *Phys. Rev. D* **108**, 024043 (2023), arXiv:2212.09655 [gr-qc].

[29] L. Pompili, E. Maggio, H. O. Silva, and A. Buonanno, Parametrized spin-precessing inspiral-merger-ringdown waveform model for tests of general relativity, *Phys. Rev. D* **111**, 124040 (2025), arXiv:2504.10130 [gr-qc].

[30] Y. Dong, Z. Wang, H.-T. Wang, J. Zhao, and L. Shao, A practical Bayesian method for gravitational-wave ringdown analysis with multiple modes, (2025), arXiv:2502.01093 [gr-qc].

[31] H.-T. Wang, G. Yim, X. Chen, and L. Shao, Gravitational Wave Ringdown Analysis Using the F -statistic, *Astrophys. J.* **974**, 230 (2024), arXiv:2409.00970 [gr-qc].

[32] K. Chandra and J. Calderón Bustillo, Black-hole ringdown analysis with inspiral-merger informed templates and limitations of classical spectroscopy, (2025), arXiv:2509.17315 [gr-qc].

[33] B. P. Abbott *et al.* (LIGO Scientific, Virgo), Tests of general relativity with GW150914, *Phys. Rev. Lett.* **116**, 221101 (2016), [Erratum: *Phys. Rev. Lett.* 121, 129902 (2018)], arXiv:1602.03841 [gr-qc].

[34] B. P. Abbott *et al.* (LIGO Scientific, Virgo), Tests of General Relativity with the Binary Black Hole Signals from the LIGO-Virgo Catalog GWTC-1, *Phys. Rev. D* **100**, 104036 (2019), arXiv:1903.04467 [gr-qc].

[35] R. Abbott *et al.* (LIGO Scientific, Virgo), Tests of general relativity with binary black holes from the second LIGO-Virgo gravitational-wave transient catalog, *Phys. Rev. D* **103**, 122002 (2021), arXiv:2010.14529 [gr-qc].

[36] R. Abbott *et al.* (LIGO Scientific, VIRGO, KAGRA), Tests of General Relativity with GWTC-3, *Phys. Rev. D* **112**, 084080 (2025), arXiv:2112.06861 [gr-qc].

[37] R. Abbott *et al.* (LIGO Scientific, Virgo), GW190521: A Binary Black Hole Merger with a Total Mass of  $150M_{\odot}$ , *Phys. Rev. Lett.* **125**, 101102 (2020), arXiv:2009.01075 [gr-qc].

[38] R. Abbott *et al.* (LIGO Scientific, Virgo), Properties and Astrophysical Implications of the  $150 M_{\odot}$  Binary Black Hole Merger GW190521, *Astrophys. J. Lett.* **900**, L13 (2020), arXiv:2009.01190 [astro-ph.HE].

[39] H. Siegel, M. Isi, and W. M. Farr, Ringdown of GW190521: Hints of multiple quasinormal modes with a precessional interpretation, *Phys. Rev. D* **108**, 064008 (2023), arXiv:2307.11975 [gr-qc].

[40] A. G. Abac *et al.* (LIGO Scientific, VIRGO, KAGRA), GW231123: a Binary Black Hole Merger with Total Mass 190-265  $M_{\odot}$ , (2025), arXiv:2507.08219 [astro-ph.HE].

[41] H. Siegel, N. M. Khusid, M. Isi, and W. M. Farr, GW231123 ringdown: interpretation as multimodal Kerr signal, (2025), arXiv:2511.02691 [gr-qc].

[42] M. Isi, M. Giesler, W. M. Farr, M. A. Scheel, and S. A. Teukolsky, Testing the no-hair theorem with GW150914, *Phys. Rev. Lett.* **123**, 111102 (2019), arXiv:1905.00869 [gr-qc].

[43] M. Giesler, M. Isi, M. A. Scheel, and S. Teukolsky, Black Hole Ringdown: The Importance of Overtones, *Phys. Rev. X* **9**, 041060 (2019), arXiv:1903.08284 [gr-qc].

[44] M. Giesler *et al.*, Overtones and nonlinearities in binary black hole ringdowns, *Phys. Rev. D* **111**, 084041 (2025), arXiv:2411.11269 [gr-qc].

[45] C. Pacilio, S. Bhagwat, F. Nobile, and D. Gerosa, Flexible mapping of ringdown amplitudes for nonprecessing binary black holes, *Phys. Rev. D* **110**, 103037 (2024), arXiv:2408.05276 [gr-qc].

[46] L. Magaña Zertuche *et al.*, High-precision ringdown surrogate model for nonprecessing binary black holes, *Phys. Rev. D* **112**, 024077 (2025), arXiv:2408.05300 [gr-qc].

[47] B. Zackay, T. Venumadhav, J. Roulet, L. Dai, and M. Zaldarriaga, Detecting gravitational waves in data with non-stationary and non-Gaussian noise, *Phys. Rev. D* **104**, 063034 (2021), arXiv:1908.05644 [astro-ph.IM].

[48] A. Correia and C. D. Capano, Sky marginalization in black hole spectroscopy and tests of the area theorem, *Phys. Rev. D* **110**, 044018 (2024), arXiv:2312.15146 [gr-qc].

[49] A. G. Abac *et al.* (KAGRA, Virgo, LIGO Scientific), GW250114: Testing Hawking's Area Law and the Kerr Nature of Black Holes, *Phys. Rev. Lett.* **135**, 111403 (2025), arXiv:2509.08054 [gr-qc].

[50] Black Hole Spectroscopy and Tests of General Relativity with GW250114, (2025), arXiv:2509.08099 [gr-qc].

[51] J. Aasi *et al.* (LIGO Scientific), Advanced LIGO, *Class. Quant. Grav.* **32**, 074001 (2015), arXiv:1411.4547 [gr-qc].

[52] F. Acernese *et al.* (VIRGO), Advanced Virgo: a second-generation interferometric gravitational wave detector, *Class. Quantum Grav.* **32**, 024001 (2015), arXiv:1408.3978 [gr-qc].

[53] Y. Aso, Y. Michimura, K. Somiya, M. Ando, O. Miyakawa, T. Sekiguchi, D. Tatsumi, and H. Yamamoto (KAGRA), Interferometer design of the KAGRA gravitational wave detector, *Phys. Rev. D* **88**, 043007 (2013), arXiv:1306.6747 [gr-qc].

[54] V. Varma, S. E. Field, M. A. Scheel, J. Blackman, D. Gerosa, L. C. Stein, L. E. Kidder, and H. P. Pfeiffer, Surrogate models for precessing binary black hole simulations with unequal masses, *Phys. Rev. Research.* **1**, 033015 (2019), arXiv:1905.09300 [gr-qc].

[55] A. Correia, Y.-F. Wang, J. Westerweck, and C. D. Capano, Low evidence for ringdown overtone in GW150914 when marginalizing over time and sky location uncertainty, *Phys. Rev. D* **110**, L041501 (2024), arXiv:2312.14118 [gr-qc].

[56] M. A. Scheel *et al.*, The SXS collaboration's third catalog of binary black hole simulations, *Class. Quant. Grav.* **42**, 195017 (2025), arXiv:2505.13378 [gr-qc].

[57] P. Arnaudo, J. Carballo, and B. Withers, Beyond quasinormal modes: a complete mode decomposition of black

hole perturbations, (2025), [arXiv:2510.18956 \[gr-qc\]](https://arxiv.org/abs/2510.18956).

[58] R. Abbott *et al.* (LIGO Scientific, Virgo), Open data from the first and second observing runs of Advanced LIGO and Advanced Virgo, *SoftwareX* **13**, 100658 (2021), [arXiv:1912.11716 \[gr-qc\]](https://arxiv.org/abs/1912.11716).

[59] R. Abbott *et al.* (KAGRA, VIRGO, LIGO Scientific), Open Data from the Third Observing Run of LIGO, Virgo, KAGRA, and GEO, *Astrophys. J. Suppl.* **267**, 29 (2023), [arXiv:2302.03676 \[gr-qc\]](https://arxiv.org/abs/2302.03676).

[60] A. G. Abac *et al.* (LIGO Scientific, VIRGO, KAGRA), Open Data from LIGO, Virgo, and KAGRA through the First Part of the Fourth Observing Run, (2025), [arXiv:2508.18079 \[gr-qc\]](https://arxiv.org/abs/2508.18079).

[61] C. M. Biwer, C. D. Capano, S. De, M. Cabero, D. A. Brown, A. H. Nitz, and V. Raymond, Pycbc inference: A python-based parameter estimation toolkit for compact binary coalescence signals, *Publications of the Astronomical Society of the Pacific* **131**, 024503 (2019).

[62] J. S. Speagle, dynesty: a dynamic nested sampling package for estimating Bayesian posteriors and evidences, *Monthly Notices of the Royal Astronomical Society* **493**, 3132 (2020), <https://academic.oup.com/mnras/article-pdf/493/3/3132/32890730/staa278.pdf>.

[63] H. Zhu *et al.*, Black hole spectroscopy for precessing binary black hole coalescences, *Phys. Rev. D* **111**, 064052 (2025), [arXiv:2312.08588 \[gr-qc\]](https://arxiv.org/abs/2312.08588).

[64] H. Yang, K. Yagi, J. Blackman, L. Lehner, V. Paschalidis, F. Pretorius, and N. Yunes, Black hole spectroscopy with coherent mode stacking, *Phys. Rev. Lett.* **118**, 161101 (2017), [arXiv:1701.05808 \[gr-qc\]](https://arxiv.org/abs/1701.05808).